INTERNATIONAL JOURNAL OF CHEMICAL REACTOR ENGINEERING

Volume 3 2005 *Article* A1

Heat Transfer in a Membrane Assisted Bubbling Fluidized Bed with Immersed Horizontal Tubes

Salim A.R.K. Deshmukh[*] Sander Volkers[†]

Martin van Sint Annaland[‡] Hans Kuipers[**]

[*]University of Twente, salim_deshmukh@yahoo.com

[†], SanderVolkers@yahoo.co.uk

[‡]University of Twente, m.vansintannaland@utwente.nl

[**]University of Twente, j.a.m.kuipers@utwente.nl

ISSN 1542-6580

Heat Transfer in a Membrane Assisted Bubbling Fluidized Bed with Immersed Horizontal Tubes

Salim A.R.K. Deshmukh, Sander Volkers, Martin van Sint Annaland, and Hans Kuipers

Abstract

The effect of gas permeation through horizontally immersed membrane tubes on the heat transfer characteristics in a membrane assisted fluidized bed operated in the bubbling fluidization regime was investigated experimentally. Local time-averaged heat transfer coefficients from copper tubes arranged in a staggered formation with the membrane tubes to the fluidized bed were measured in a square bed (0.15 m x 0.15 m x 0.95 m). Glass particles (75-110 micrometer) were fluidized with air distributed via a porous plate, where the ratio of gas fed or removed through the membrane bundles and the porous plate distributor was varied. The experimental results revealed that high gas permeation rates through the membranes strongly decreased the heat transfer coefficient at high superficial gas velocities for tubes at the top of the tube bundle, which was attributed to the reduced mobility and increased bubble hold up and/or dilution of the emulsion phase, reducing overall heat capacity.

In the design of membrane assisted fluidized beds care must be taken to include the effect of gas addition or withdrawal through the membranes on the required heat transfer surface area.

KEYWORDS: Membrane assisted fluidized bed, membranes, permeation and tube-to-bed heat transfer.

1. INTRODUCTION

Fluidized beds employing fine powders are finding increased application in the chemical and petrochemical industry because of their excellent mass and heat transfer characteristics. However, in fluidized bed chemical reactors axial gas back-mixing can strongly decrease the conversion and product selectivities. By insertion of membranes in fluidized beds large improvements in conversion and selectivity can be achieved, firstly by optimizing axial concentration profiles via distributive feeding of one of the reactants or selective withdrawal of one of the products, and secondly, by decreasing the effective axial dispersion via compartmentalization of the fluidized bed. Moreover, insertion of membrane bundles in a suitable configuration impedes bubble growth, thereby reducing reactant by-pass via rapidly rising large bubbles. Often cooling or heating tubes are also submerged in the fluidized bed to withdraw or add thermal energy respectively. The effective heat transfer coefficient between the surface of these tubes and the fluidized bed is an important parameter in the design of these fluidized beds. The integrated gas addition or removal via membranes inside the fluidized bed strongly influences the bed hydrodynamics and thus the tube-to-bed heat transfer.

Numerous previous studies have been carried out to study various aspects of tube-to-bed heat transfer in fluidized beds. However, studying the tube-to-bed heat transfer in a membrane assisted fluidized bed is novel and has never been done before, to the author's knowledge. In this work the influence of the presence of membrane and heat transfer tube bundles and the effect of gas addition and removal via the membrane tubes, on the spatial distribution of the time averaged tube-to-bed heat transfer coefficient in a bubbling fluidized bed at various fluidization velocities was studied experimentally.

Before presenting and discussing experimental results, first the experimental set-up, the experimental technique and experimental procedure used to measure the tube-to-bed heat transfer coefficient are described in the next section. Finally the experimental data is compared with literature correlations.

2. EXPERIMENTAL

A very high specific membrane surface area can be achieved with membrane tubes of very small tube diameter. However, to accomplish the desired heat exchange to withdraw the released reaction heat or to supply the required reaction energy, heat transfer tubes of similar small size are required. A membrane assisted fluidized bed has been constructed to measure the local heat transfer coefficient consisting of membranes and heat transfer tubes of comparable tube diameter of about 3 mm. Moreover, small heat transfer tubes allow an accurate measurement of the tube-to-bed heat transfer coefficients by reducing the heat transfer resistance inside the heat transfer tubes as explained in section 2.2 and difficulties in the interpretation of the results due to the curvature effect of the heat transfer tubes can be avoided.

First the membrane assisted fluidized bed and the arrangement of the inserts is explained. Subsequently the experimental technique to measure tube-to-bed heat transfer coefficient is explained with special attention to the particle electrostatic effects on the tube-to-bed heat transfer coefficient.

2.1 Experimental set-up

To measure the spatial distribution of the heat transfer coefficient, a square fluidized bed (0.15 m x 0.15 m x 0.95 m) was constructed out of lexan and filled with glass beads (75-110 μm, 2550 kg/m^3) to a packed bed height of about 0.30 m. The bed was equipped with 18 horizontal copper heat transfer tubes (2 mm ID and 3 mm OD) and 40 horizontal ceramic membrane tubes (1.5 mm ID and 2.5 mm OD with a pore size of 0.15 μm and scarcely permselective), through which gas could be added or withdrawn, arranged in a staggered orientation with an equilateral pitch of 0.02 m. In Figure 1 top view of the membrane assisted fluidized bed and schematic side view of the tube arrangement is shown. Uniform fluidization was achieved with a porous plate distributor with a pore size of 10 μm. Fluidization was performed with humidified air (50-60 % humidity) at ambient conditions to avoid static electricity problems (see Figure 2).

It was found that static charging of the particles strongly decreased the measured heat transfer coefficients, especially in experiments with tube bundles submerged in the bed. Furthermore, it was verified experimentally that the bed temperature was uniform throughout the bed.

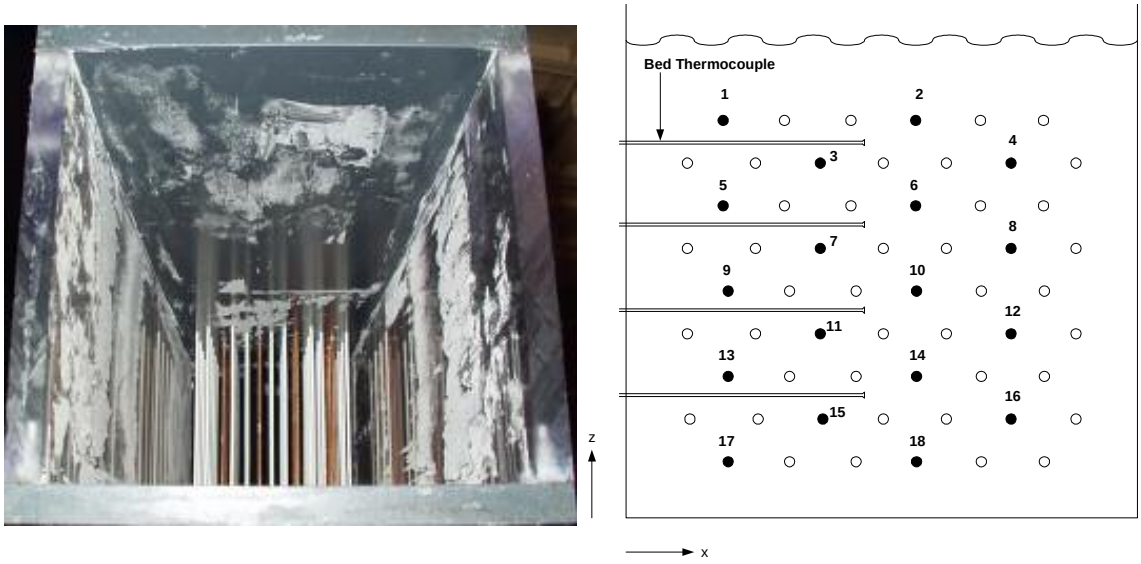

(a) Top view (b) Side view

Figure 1. Picture (top view) and schematic side view of the membrane assisted fluidized bed; •: Heating tube, o: Membrane tube.

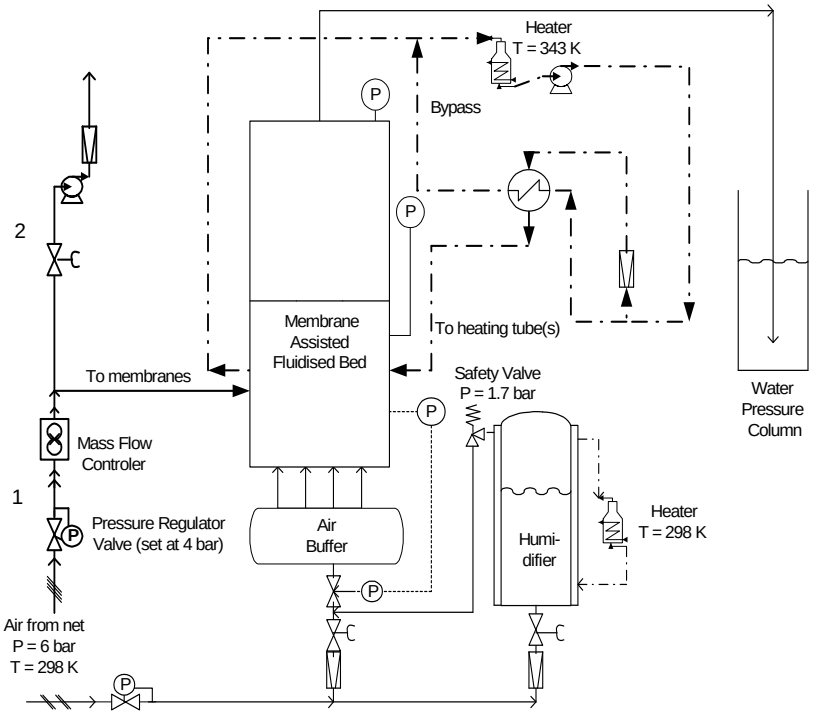

1: gas addition, 2: gas withdrawal

Figure 2. Schematic of the experimental set-up.

2.2 Experimental technique

Various experimental methods have been reported in the literature to measure the heat transfer coefficient between a submerged surface and the fluidized bed. The most frequently reported method is an electrically heated metallic film sensor (e.g. Tout and Clift, 1973 and Fitzgerald et al., 1981). This method is based on the change in the resistance of a metallic film with temperature. The film is heated to a certain temperature, which is different from the bed temperature, and kept constant by varying the power supplied to the film using a thermocouple or a reference resistance. Based on this principle, it is also possible to use long strips and measure along a surface. The problem of this method was that the metallic films were relatively large compared to the tube size used.

A method based on thermocouples was used by George (1987), by Olsson and Almsted (1992), and by McKain et al. (1994). The advantage of using thermocouples as sensors is the relatively small area of the thermocouples, the low price, the commercial availability and easiness of construction. By using at least two thermocouples at different radial positions on the outer surface of the tube, information on bubble passage can be obtained. Again, heat transfer coefficients between the bed and the heat transfer tubes of very small size (3 mm) studied in this work cannot be measured with this method.

Karamavruc et al. (1994) and Kahn and Turton (1992) have used an experimental technique that only requires one thermocouple. The principle of the technique is that a thermocouple is positioned at the outside surface of a tube and that the inside temperature is kept at a constant value. This can be accomplished by using a very high water flow rate. A disadvantage of this method is that the thermocouple is incorporated in the tube, as is the case in the multiple thermocouple method. This means that every single tube has to have one thermocouple fitted at the surface. Furthermore, the temperature difference between the water at the inside and particles at the outside of the tube has to be considerable in order to accurately measure the heat transfer coefficient.

In this work the tube-to-bed heat transfer coefficient was determined by measuring the difference between the entrance and the exit mixing-cup temperatures of the heat transfer fluid, which was preheated water, fed with an average velocity of 4.6 cm/s at about 50 °C and the bed temperature using T-type thermocouples. An accurate measurement of the mixing cup temperature was ensured by positioning static mixers inside the tube (see Figure 3) and averaging over 2 to 5 minutes. An advantage of this technique to measure the heat transfer coefficient is that the thermocouples can be switched easily from one tube to another to determine the axial and lateral variation of the heat transfer coefficient in the bed.

A thermal energy balance over a single heat transfer tube submerged in the fluidized bed reads:

$$\phi_m C_p \frac{dT_{water}}{dz} = \pi d_i h_{total} \left(T_{water} - T_{bed} \right) \tag{1}$$

where the overall heat transfer coefficient, h_{total}, is given by:

$$\frac{1}{h_{total}} = \frac{1}{h_{tube}} + \frac{d_i \, ln(\frac{d_o}{d_i})}{2\lambda_{copper}} + \frac{1}{h_{bed}} \frac{d_i}{d_o} \tag{2}$$

Assuming constant physical properties and a constant bed temperature in the fluidized bed, $Nu = h_{tube} d_i / \lambda_{water} = 3.66$, i.e. $h_{tube} \cong 1150$ $Wm^{-2}k^{-1}$, can be taken for the heat transfer resistance in the hydrodynamically and thermally fully developed laminar flow inside the copper heat transfer tubes, as can be deduced from the measured axial temperature profile inside the heating tube (see Figure 4). With this technique the time averaged tube-to-bed heat transfer coefficient could be determined well within a maximum experimental error of 10% with good reproducibility, provided that the fluidizing air was sufficiently humidified (see Figure 5) to avoid effects induced by electrostatic forces.

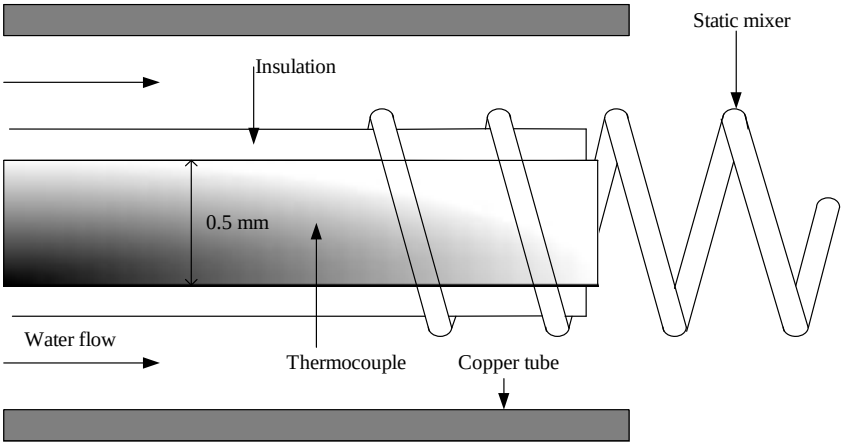

Figure 3. Schematic of the thermocouple arrangement in the tube for measuring the mixing cup temperature.

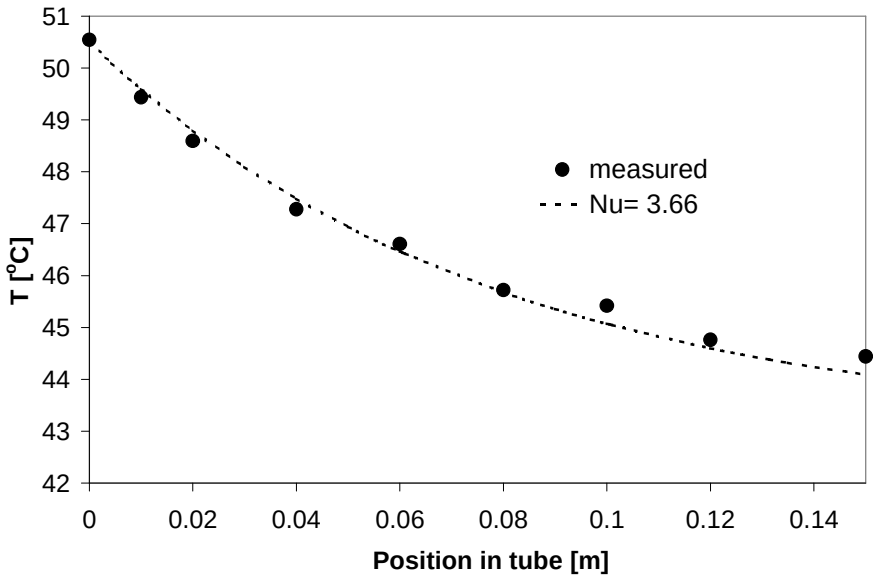

Figure 4. Experimental verification of water temperature profile inside the heat transfer tube.

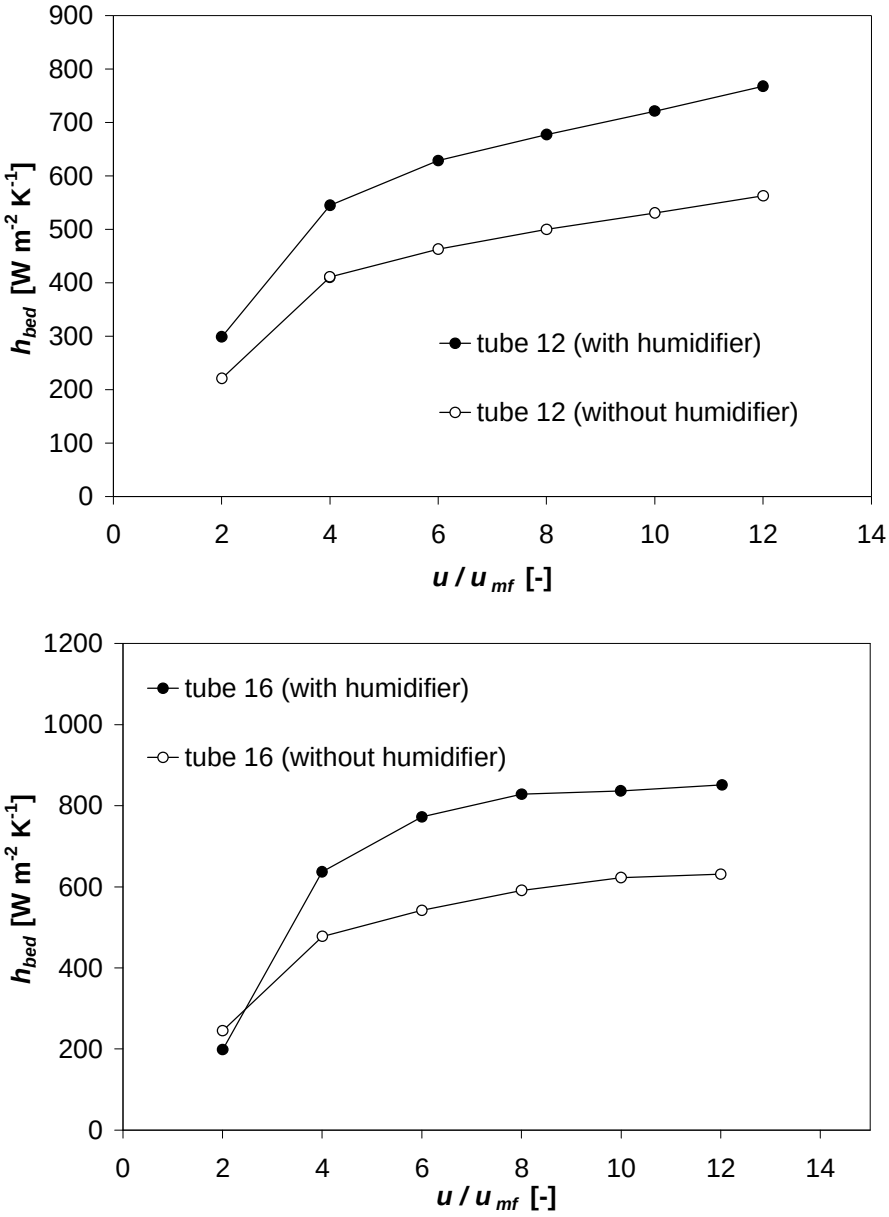

Figure 5. Static electricity effect on experimentally measured tube-to-bed heat transfer coefficient.

3. EXPERIMENTAL RESULTS AND DISCUSSION

Firstly, experimental results for the time averaged tube-to-bed heat transfer coefficient for a single tube are presented and compared with reported experimental values in the literature. Subsequently, the results for tube banks without permeation through the membranes will be reported. Finally, the effect of permeation through the membranes will be discussed.

3.1 Heat transfer from a single tube

The heat transfer coefficient between the surface of a single tube submerged in a fluidized bed was measured at different positions in the fluidized bed in order to compare the observed heat transfer coefficients with reported literature values and as a reference for the experiments employing tube-banks. The experimentally determined tube-to-bed heat transfer coefficient increased with increasing superficial gas velocities and reached a maximum at about $8u_{mf}$. The maximum tube-to-bed heat transfer coefficient (h_{max}) increased as a function of height above the distributor (tube 16: 830 W/m^{2}K; tube 2: 970 W/m^{2}K; (see Figure 1b)), which is attributed to increased solids mobility higher in the bed due to bubble coalescence. In the lateral direction no significant changes in the heat transfer coefficient were observed even at high superficial gas velocities. Wall effects were not measured since the measurement closest to the wall was 1.7 cm.

3.2 Heat transfer with a tube bank without membrane permeation

The tube-to-bed heat transfer coefficients were measured in the fluidized bed for all the 18 tubes placed in the bed at different superficial gas velocities without permeation through the membrane tubes. As shown in Figure 6, the measured heat transfer coefficient increases with the superficial gas velocity and levels off at higher gas velocities to a maximum. Increasing the superficial gas velocity increases the mobility of the emulsion phase, which decreases the average residence time of an emulsion phase ‘packet’ at the tube surface, thereby increasing the heat transfer coefficient. However, at higher gas velocities more and larger bubbles are formed having a lower volumetric heat capacity, causing the heat transfer coefficient to level off and eventually decrease at very high gas velocities (see e.g. Kunii and Levenspiel, 1991). Furthermore, the heat transfer coefficient strongly decreases as a function of the distance from the distributor, caused by the bubble growth and coalescence.

When comparing the maximum heat transfer coefficient determined in the fluidized bed with a tube bank with the results obtained with a single tube, the tube-to-bed heat transfer coefficient decreased by almost 200 W/m^{2}K (see Figure 6 b) due to the reduced mobility of the emulsion phase caused by the additional internals, which obstruct the macro-scale movement of the emulsion phase. Moreover, the internals promote bubble breakage, which reduces the bubble rise velocity, resulting in decreased emulsion movement in the vicinity of the heat transfer surfaces.

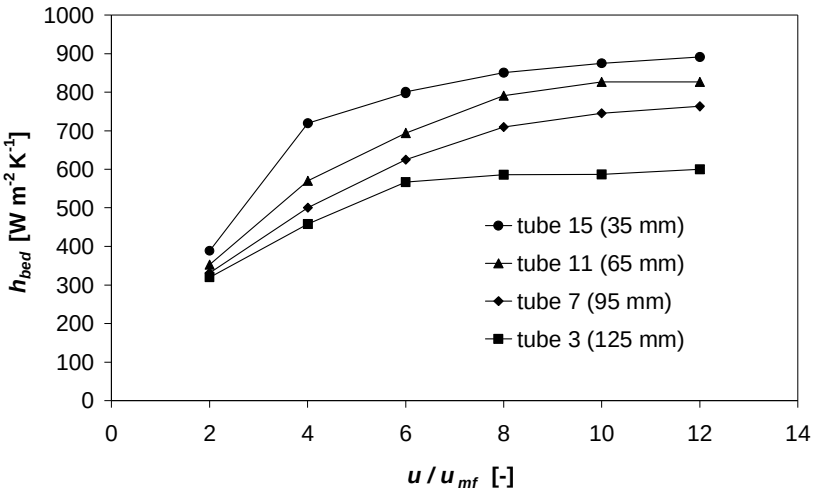

(a)

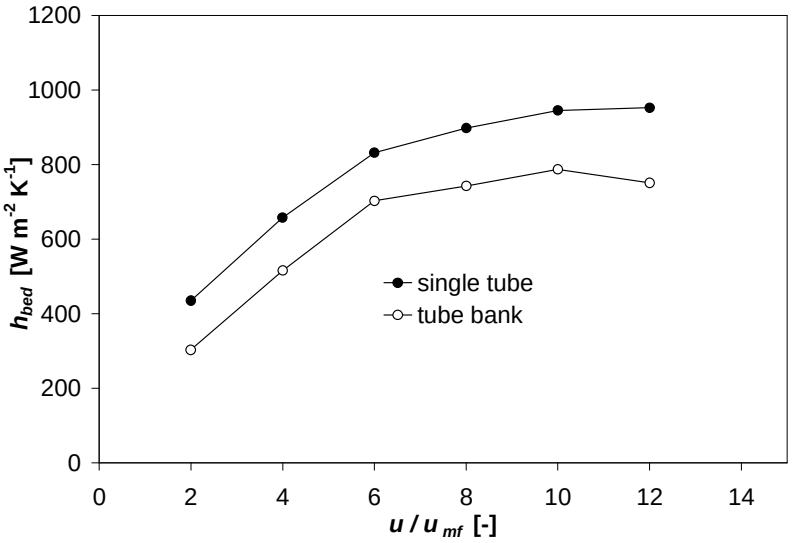

(b)

Figure 6. Tube-to-bed heat transfer coefficient as a function of the superficial gas velocity; a) for different heights above the distributor (Tube number refers to position indicated in Figure 1); b) for an experiment with a single tube and a tube bank, measured at position 2.

In Figure 7 the spatial distribution of the heat transfer coefficient for two different superficial gas velocities is shown. Increasing the superficial gas velocity from $6u_{mf}$ to $10u_{mf}$ increases the tube-to-bed heat transfer coefficient, but does not change its spatial distribution. The highest heat transfer coefficients were observed just above the distributor in the center of the bed. A slight lateral asymmetry in the spatial distribution is caused by the asymmetric configuration of the heat transfer tubes.

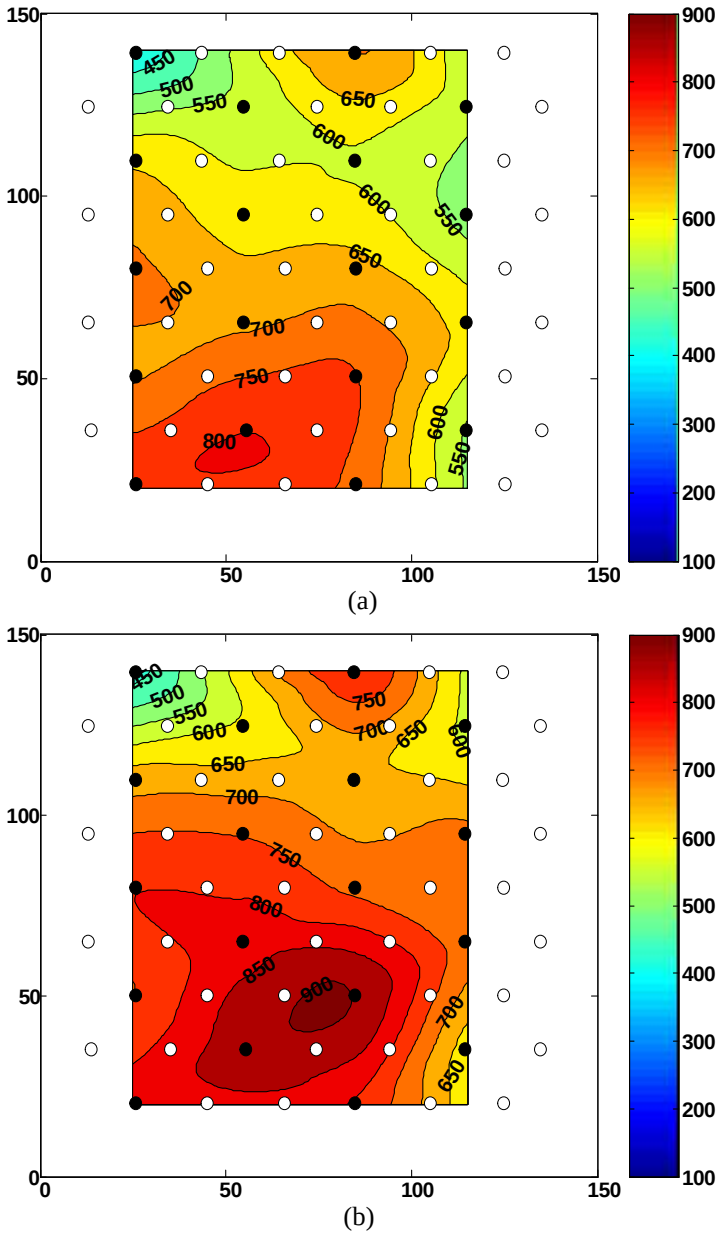

Figure 7. Spatial distribution of the tube-to-bed heat transfer coefficient for two different superficial gas velocities; (a) 6 u_{mf} and (b) 10 u_{mf}.

3.3 Heat transfer with a tube bank with membrane permeation

To study the effect of gas permeation via membranes on the tube-to-bed heat transfer coefficient, experiments were carried out by adding or removing part of the fluidizing gas via the membranes at different superficial gas velocities. Up to 40% of the total gas flow could be added via the membranes, whereas only 10% of the total gas flow could be removed due to pump limitations. In the experiments where gas was added through the membranes, the total gas feed was kept constant, which implies that experiments with higher permeation rates through the membranes were carried out at a lower gas flow through the distributor.

3.3.1 Effect of membrane permeation on heat transfer coefficient

In Figure 8 the spatial distribution of the tube-to-bed heat transfer coefficient is given at an overall superficial gas velocity of $6u_{mf}$ for different ratios of gas fed via the membranes relative to the total gas flow rate. The Figure clearly shows that with increasing gas permeations through the membrane the measured heat transfer coefficient at the bottom of the bed decreases and that the heat transfer coefficient decreases in a much more pronounced way as a function of the axial position in the bed. The lower heat transfer coefficient at the bottom of the bed at higher gas permeations was caused firstly by the lower gas feed through the distributor and secondly by the suppressed macroscopic circulation pattern due to the reduced down flow at the walls and the reduced bubble growth in the centre of the bed. Furthermore, the heat transfer coefficient decreases strongly as a function of the height above the distributor and even much more pronounced than observed for the experiment without permeation, where the decrease in the heat transfer coefficient was caused by the bubble growth. The additional decrease in the heat transfer coefficient as a function of the axial coordinate is attributed to an increased bubble hold-up due to the smaller average bubble diameter and the dilution of the emulsion phase in case part of the gas is fed via the membranes, which results in a decreased volume and heat capacity of the emulsion phase.

3.3.2 Effect of superficial gas velocity on heat transfer coefficient

Figure 9 depicts the effect of the superficial gas velocity on the tube-to-bed heat transfer coefficient at different permeations and at two different tube locations. For a tube located at the top of the bed, the effect of membrane permeation on the tube-to-bed heat transfer coefficient was negligible at a low fluidization velocity of $2u_{mf}$, but very strong at higher gas velocities (see Figure 9 a). At a low superficial gas velocity the emulsion packet renewal rate at the tube surface was very low due to the absence of a large macroscopic circulation pattern caused by the absence of larger bubbles. Hence, the tube-to-bed heat transfer coefficient will mainly depend on the local superficial gas velocity. Remarkably, at high gas permeations through the membrane an increase in the total gas flow does not increase the heat transfer coefficient for a tube at the top of the bundle. The increased macroscopic emulsion circulation at higher gas velocities (because of the larger bubbles) is more than counterbalanced by the increased bubble hold-up and/or dilution of the emulsion phase.

For a tube in the center of the bed the effect of permeation through the membranes is very pronounced at a low fluidization velocity of $2u_{mf}$ (see Figure 9 b) because of the reduced local gas velocity at higher permeation rates. However, at high superficial gas velocities only a small decrease in the heat transfer coefficient at higher membrane permeations was observed, because of the smaller local effect on the bubble hold-up and/or dilution of the emulsion phase, since the tube in the center of the tube bundle experiences only part of the total gas fed via membranes.

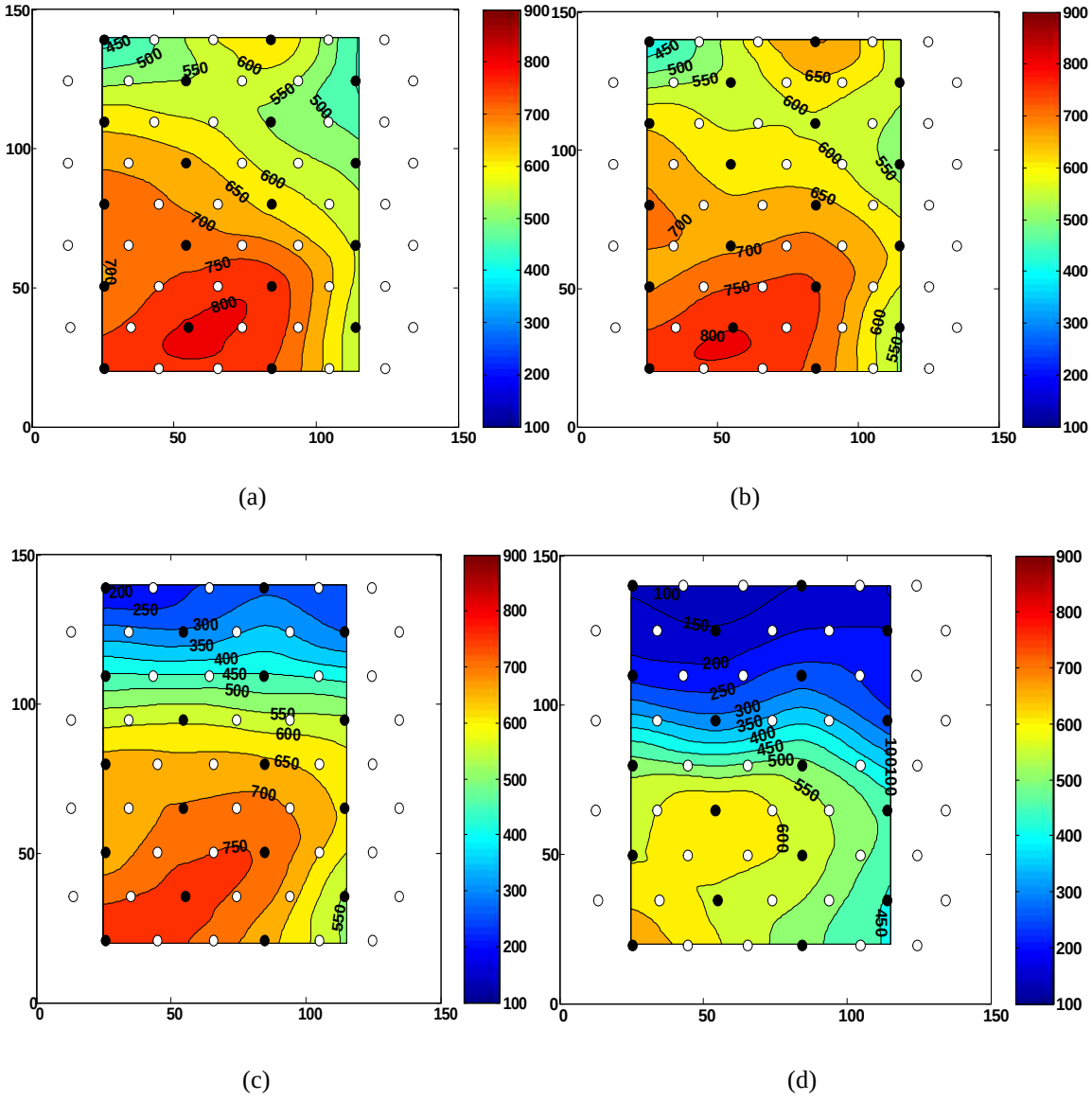

Figure 8. Heat transfer coefficients of the bed at various positions in the bed at 6 u_{mf}; a) -10 % permeation; b) no permeation; c) 20% permeation; d) 40% permeation. % Permeation: fraction of the total gas added or removed via the membranes

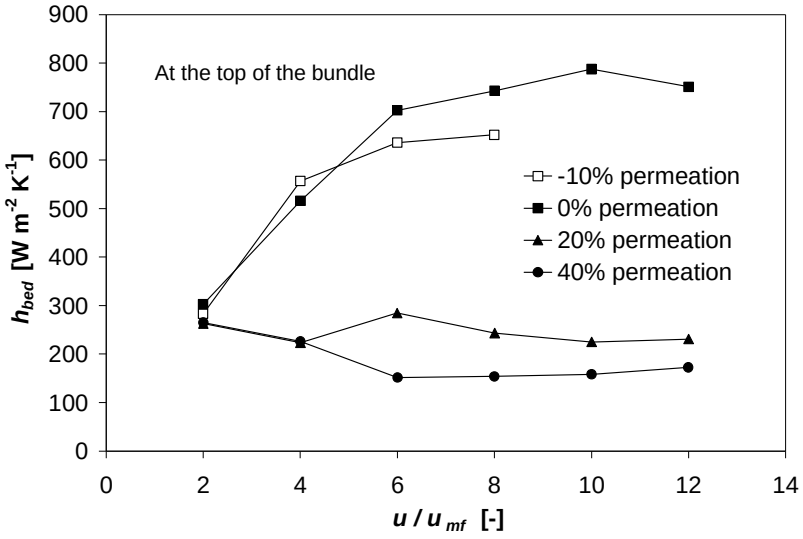

(a)

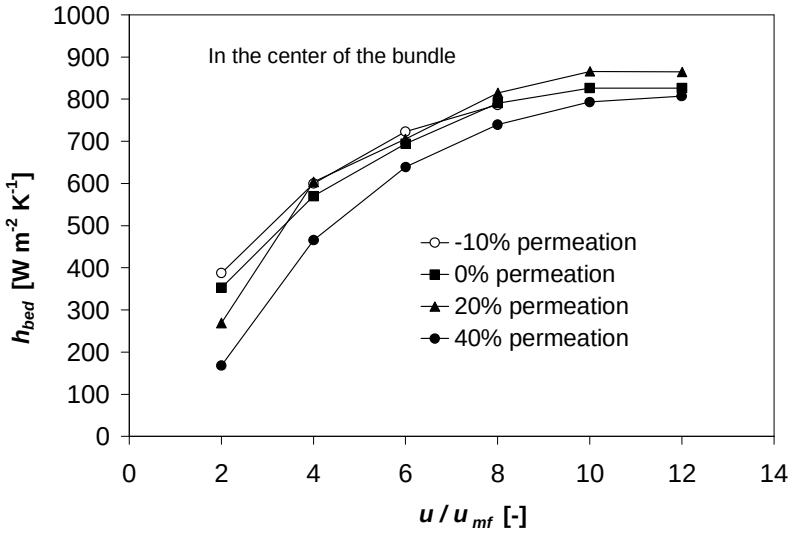

(b)

Figure 9. Tube-to-bed heat transfer coefficient as a function of the superficial gas velocity; a) Tube position 2 (top of the tube bundle); b) Tube position 11 (center of the tube bundle).

4. COMPARISON WITH LITERATURE CORRELATIONS

In this section the experimental results for the tube-to-bed heat transfer coefficient are compared with experimental data from the literature. Then, these values are compared with various correlations for the tube-to-bed heat transfer coefficients, only for the case of a membrane assisted fluidized bed without membrane permeation, since the effect of membrane permeation has not been accounted for in these correlations.

The measured tube-to-bed heat transfer coefficients compare well with experimental values reported in the literature, which were measured with heat transfer probes for similar systems under comparable fluidization conditions (Sharma, 1997 and Sharma and Turton, 1998) (see Table 1).

Table 1. Experimentally determined heat transfer coefficients for a single tube submerged in a fluidized bed without inserts reported in the literature for similar system under comparable fluidization conditions

Material	d_p (μm)	h_{max} ($W \cdot m^{-2} \cdot K^{-1}$)	h_{avg} ($W \cdot m^{-2} \cdot K^{-1}$)	Reference
Glass	76	-	766	Sharma, 1997
Glass	76	-	825	Sharma and Turton, 1998
Glass	100	850	-	Sharma and Turton, 1998

The experimentally determined tube-to-bed heat transfer coefficients for the tube bank without membrane permeation through the membranes are compared with the literature correlations (see table 2).

All correlations (except Molerus et al., 1995) determine a maximum heat transfer coefficient. For the current experiment investigation the heat transfer coefficient at $12u_{mf}$ was used as an approximation for the maximum heat transfer coefficient. At $12u_{mf}$ the average heat transfer coefficient of the bed was experimentally found to be about 800 W/m^2 K. The macroscopic relations all underestimate h_{bed}. Especially the correlation of Grewal and Saxena grossly underestimates h_{bed} (about 600%). The correlation by Prins et al. (1989) also gives a too low value of the heat transfer coefficient, but only about 25%. In Figure 10, the experimental results of tube 8 are compared with the results of the correlation of Molerus et al. (1995). It predicts much lower values for h_{bed} than experimentally found.

The mesoscopic models give a better prediction of the maximum heat transfer coefficient. The mesoscopic models resemble the macroscopic models; only more detailed knowledge of the fluidised bed is needed. This model incorporates bed parameters such as the bubble frequency, the thickness of a stagnant particle or gas layer or the bubble fraction. In literature, two types of models can be found. The first type of model is based on the gas-film resistance (e.g., Martin, 1984a, and Molerus, 1997). It assumes that the heat transfer is governed by the resistance in a thin gas film around the surface. The second type of model is the packet renewal model, which was first derived by Mickley and Fairbanks (1955). This model assumes that the heat transfer takes place via emulsion packets at the surface, which are replaced when a bubble passes. The correlation of Chandran and Chen (1983) gives the best approximation of the maximum heat transfer coefficient.

Table 2. Comparison of maximum tube-to-bed heat transfer coefficient predicted by various literature correlations

No.	Author	Correlation	h_{bed} ($W \cdot m^{-2} \cdot k^{-1}$)
1	Grewal and Saxena (1980)	$Nu_{wp,\max} = \frac{h_{bed} D_t}{k_e} = 0.9 \left(Ar \cdot \frac{D_{12.7}}{D_t} \right)^{0.21} \left(\frac{C_{p,p}}{C_{p,g}} \right)^{0.2} \left[1 - 0.21 \left(\frac{P}{D_t} \right)^{-1.75} \right]$	127
2	Prins et al. (1989)	$Nu_{wp,\max} = \frac{h_{bed} D_t}{k_e} = 4.175 \cdot Ar^{0.087 \left(D_t / d_p \right)^{0.128}} \left(0.844 + 0.0756 \left(\frac{T_{bed}}{273K} \right) \right)_T \left(\frac{D_T}{d_p} \right)^{-0.278}$	640
3	Molerus et al. (1995)	$Nu = \frac{h_{pc} l_l}{k_g} = \frac{0.125 \left(1 - \varepsilon_{mf} \right)}{1 + \frac{k_g}{2 C_p \mu}} \cdot \frac{1}{1 + 25 \left\{ \sqrt[3]{\frac{u - u_{mf}}{u_{mf}}} \sqrt[3]{\frac{\rho C_{p,p}}{k_g g}} \left(u - u_{mf} \right) \right\}^{-1}}$	550 (at $12u_{mf}$)
4	Mickley and Fairbanks (1955)	$h_{bs} = \sqrt{k_e \rho_e C_{p,e} S}$	963
5	Chandran and Chen (1983)	$Nu_e \cong \frac{2}{\sqrt{\pi}} \exp \left[-a_1 N_f^{\left(a_2 + a_3 ln \left[1/N_f \right] \right)} \right] \sqrt{N_f}$	780
6	Kunii and Levenspiel (1991)	$h_{bed} \cong \left[\frac{1 - \delta}{\frac{1}{h_{packet}}} \right]_{emulsion} = 1.13 \left[k_e^0 \rho_p (1 - \varepsilon_{mf}) C_{p,p} f \left(1 - \delta \right) \right]^{1/2}$	636

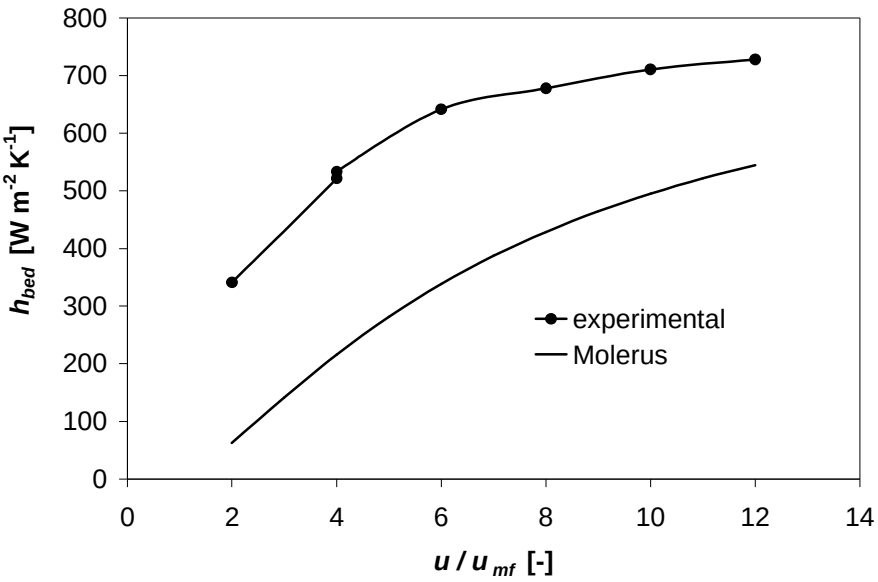

Figure 10. Comparison of experimental value of the h_{bed} with model of Molerus et al. (1995).

5. SUMMARY AND CONCLUSIONS

The effect of presence of and the gas permeation through horizontally submerged membrane tubes in a fluidized bed on the time averaged tube-to-bed heat transfer coefficient was investigated experimentally by measuring the bed temperature and the inlet and outlet mixing-cup temperatures of water flowing through heat transfer tubes.

The presence of the membrane and heat transfer tubes decreases the heat transfer coefficient due to the reduced mobility of the emulsion phase, caused by the internals obstructing the macro-scale movement of the emulsion phase, and by the enhanced bubble breakage decreasing the bubble rise velocity.

Without gas permeation through the membranes, the heat transfer coefficients increase with increasing superficial gas velocity and level off at high gas velocities to a maximum, where the increased emulsion phase mobility is counterbalanced by the larger bubbles. The heat transfer coefficient decreased as a function of the distance from the distributor, which was attributed to bubble growth due to coalescence. The experimentally determined tube-to-bed heat transfer coefficient compare reasonably well with the mesoscopic correlations from the literature for the case of no gas permeation through the membranes. At high gas permeation rates through the membranes the decrease in the heat transfer coefficient at the top of the tube bundle was even stronger at high superficial gas velocities, caused by the increased bubble hold-up and/or dilution of the emulsion phase. However, lower in the tube bundle the decrease in the heat transfer coefficient was less pronounced, since these tubes experienced only part of the total gas fed via membranes.

Concluding, in a membrane assisted fluidized bed the product selectivity and/or operational safety can be enhanced, but care must be taken to include the effect of gas addition through the membranes on the required heat transfer surface area. A direct measurement of the bubble size (distribution) and frequency using noninvasive electrical capacitance tomography (ECT) techniques or optical/capacitance probes would be interesting to support the reported experimental findings. Additionally, measurements with varying heat capacity of the emulsion phase with addition or removal of gas via the membranes are recommended, as well as experiments with different membrane tube diameters and tube pitches. Furthermore, also the effect of the fluidization conditions on the possible abrasion of the submerged membrane tubes needs further attention.

ACKNOWLEDGEMENT

This research is part of the research program carried out within the Center for Separation Technology, as cooperation between the University of Twente and TNO, the Netherlands Organization for Applied Scientific Research. The author wishes to thank W. Leppink and G. Schorfhaar for construction and maintenance of the set-up.

NOTATIONS

a	constant
Ar	Archimedes number $\left(\frac{d_p^3 \rho_g \left(\rho_s - \rho_g\right) g}{\mu_g^2} \right)$
C_p	heat capacity [J·kg^{-1}·K^{-1}]
d	diameter of the copper tube [m]
d_p	diameter of the particle [m]
D	tube diameter [m]
f	bubble frequency [s^{-1}]
g	gravitational acceleration [m·s^{-2}]
h	heat transfer coefficient [W·m^{-2}·K^{-1}]
h_{bed}	bed heat transfer coefficient [W·m^{-2}·K^{-1}]
h_{total}	overall heat transfer coefficient [W·m^{-2}·K^{-1}]
h_{tube}	tube side heat transfer coefficient [W·m^{-2}·K^{-1}]
k	thermal conductivity [W·m·K^{1}]
$k_e^{\,0}$	thermal conductivity at minimum fluidization [W·m·K^{1}]
l_l	laminar flow length scale [m]
N_f	number frequency
P	pitch [m]
S	stirring factor
T	temperature (°C)
u	Superficial gas velocity [m·s^{-1}]
u_{mf}	minimum fluidization velocity [m·s^{-1}]
v_{av}	average velocity of water in the tube [m·s^{-1}]
Z	tube length [m]
Nu	Nusselt number $\left(h_{bed} d_o / \lambda \right)$

Greek letters

ε	voidage
ϕ_m	mass flow rate of water [kg·s^{-1}]
λ_{copper}	thermal conductivity of copper [W·m·K^{1}]
λ_{water}	thermal conductivity of water [W·m·K^{1}]
ρ	density of water [kg·m^{-3}]
μ	viscosity [Pa·s]
δ	bubble fraction

Subscripts

avg	average
bs	bed to surface
e	emulsion phase
g	gas phase
i	inside
max	maximum

mf	minimum fluidization
o	outside
p	particle
pc	particle convection
t,T	tube
wp	particle to wall

REFERENCES

Chandran, R. and Chen, J.C., "A heat transfer model for tubes immersed in gas fluidized beds", AICHE J. 31, 244 (1983).

Fitzgerald, T.J., Catipovic, N.M. and Jovanovic, G. N., "Instrumented cylinder for studying heat transfer to immersed tubes in fluidized beds", Ind. Eng. Chem. Fund. 20, 82-88 (1981).

George, A.H., "A transducer for the measurement of instantaneous local heat flux to surfaces immersed in high temperature fluidized beds", Int. J. Heat. Mass. Transfer, 30 (4), 763-769 (1987).

Grewal, N. S. and Saxena, S. C., Ind. Eng. Chem. Proc. Dev., 20, 109-116 (1980).

Kahn, T. and Turton, R., "The measurement of instantaneous heat transfer coefficients around the circumference of a tube immersed in a high temperature fluidized bed", J. Heat Mass Transfer, 35 (12), 3397-3406 (1992).

Karamavruc, A.I., Clark, N.N. and McKain, D.L., "Deduction of fluidized bed heat transfer coefficients using one- and two-dimensional analyses", Powder Technology, 80, 83-91 (1994).

Kunii, D. and Levenspiel, O., "Fluidization Engineering, second edition", Butterworth-Heinemann series in chemical engineering, chapter 13 (1991).

McKain, D., Clark, N., Atkinson, C. and Turton, R., "Correlating local tube surface heat transfer with bubble presence in a fluidized bed", Powder Technology, 79, 69-79 (1994).

Mickley, H.S. and Fairbanks, D.F., Mechanism of Heat Transfer to Fluidized Beds, A.I.Ch.E. J., Vol. 1, No. 1. 374-384 (1955).

Molerus, O., Buschka, A. and Dietz, S, "Particle migration and heat transfer in fluidized beds- II: Prediction of heat transfer in bubbling fluidized beds", Chem. Eng. Sci. Vol.50, No. 5, 879-885 (1995).

Olsson, S.E. and Almsted, A.E., "Local instantaneous and time-averaged heat transfer in pressurized fluidized beds with horizontal tubes: influence of the pressure, fluidization velocity and tube-bank geometry", Chem. Eng. Sci., 50 (20), 3231-3245 (1992).

Prins, W., Harmsen, G. J., De Jong, P. and Van Swaaij, W.,"Heat transfer from an immersed fixed silver sphere to a gas fluidized bed of very small particles", Fluidization VI, Grace, J.R. eds., Engineering Foundation, New York, 677-684 (1989).

Sharma, K.R., "Relative contributions from particle conduction and gas convection to the heat transfer coefficient between dense gas-solid fluidized beds and surfaces", Powder Technology, 91, 75-80 (1997).

Sharma, K.R. and Turton, R., "Mesoscopic approach to correlate surface heat transfer coefficient with pressure fluctuations in dense gas solid fluidized beds", Powder Technology, 99, 109-118 (1998).

Tuot, J. and Clift, R., "Heat transfer around single bubbles in a two-dimensional fluidized bed", A.I.Ch.E.J., 69 (128), 78-84 (1973).